Hindawi
Mathematical Problems in Engineering
Volume 2018, Article ID 3242703, 10 pages
https://doi.org/10.1155/2018/3242703

Research Article

Simulation and Statistical Modeling of Acoustic Scattering of Bubble Wakes

Zhu Ling-Guo,[1,2] **Zhao An-Bang**,[1] **Wang Jin**,[2] **Ma Zhong-Cheng**,[2,3] **Cao Qing-Gang**,[2] **and Yang Bao-Shan**[2]

[1]*College of Underwater Acoustic Engineering, Harbin Engineering University, Harbin 150001, China*
[2]*Dalian Scientific Test and Control Technology Institute, Dalian 116013, China*
[3]*Science and Technology on Underwater Test and Control Laboratory, Dalian 116013, China*

Correspondence should be addressed to Zhao An-Bang; zhaoanbang@hrbeu.edu.cn

Received 11 August 2018; Accepted 2 December 2018; Published 27 December 2018

Academic Editor: Lukasz Pieczonka

Ship wakes are large, exist for a long time, and are difficult to disguise or conceal. These characteristics can be used as an important basis for ship tracking and recognition. However, distinguishing between wakes, underwater targets, and sea surface is a difficult problem that currently limits acoustic wake homing technology. To solve this problem, in this study, from the viewpoint of feature recognition, the effects of bubble radius, air volume fraction, frequency, depth, and other parameters on the group bubble were first investigated. The volume scattering intensity of acoustic wakes at different frequencies and depths was also calculated and analyzed, and the results of our theoretical calculations were verified through an experiment using a multifrequency single wave sonar dock. Subsequently, through the single frequency and multibeam sonar sea trial test, a statistical model of target characteristics with a clear physical mechanism was developed. The developed model can be utilized for the guidance and recognition of acoustic wake targets. Thus, this study lays the foundation for the practical application of acoustic wake guidance.

1. Introduction

As a type of underwater acoustic target, a bubble wake is the main source of information for detecting and identifying underwater targets by torpedoes and sonars. The tail of a ship is like the tail of a target. After the target has passed, this wake can still remain in its place for a long time. This creates a requirement for the weapon and/or equipment to be guided by a map. A torpedo, which is guided by the wake's characteristics, has good anti-interference ability, high guidance precision, high hit rate, and good damage capability [1]. Acoustic wake homing has become a major area in underwater self-guided weapon research and applications. Therefore, over the past century, research on wakes has been ongoing.

From the 60s to the 80s, the United States began to study the wake characteristics of ships on a large scale. Researchers have used the Pohl Seidman transport equation and Lagrange's method to study the dynamics of bubbles in the oceanic environment [2, 3]. Miner and Ramberg used the Navier-Stokes equation and bubble transport theory to study the bubble distribution in warship wakes [4]. Carrica et al. calculated the influence of ships on the bubble background in the ocean using a two-phase flow model [5].

During the middle and late stages of World War II, the United States measured and analyzed the acoustic characteristics of wakes of more than ten types of ships, from yachts to destroyers, conducting many measurements and compiling the results into monographs [6, 7]. After the war, torpedoes guided by acoustic wakes were successfully developed. In the 90s, the American, French, Canadian academies of Oceanographic Sciences used multifrequency sonar to measure the acoustic scattering characteristics and geometric features of wakes, as well as other physical features [8, 9].

In China, Shengwei et al. used fluid mechanics theory to study the size, density, distribution, and other characteristics of the bubble [10]. Nie et al. used the lattice Boltzmann

method to study the multibubble merging mode and increasing speed [11]. Donghua et al. used the improved Reynolds average Navier-Stokes flow model and bubble transport theory to calculate and analyze the number density (BND) distribution of the wake bubble [12]. The active acoustic characteristic model of the bubbles in the wake was established by Qun and Yingmin, and their active acoustic characteristics were analyzed. The finite element method was used to analyze the acoustic characteristics of the bubbles in the wake of warships [13].

At Harbin Engineering University, a single transducer was used to test the wake of a motorboat and a traffic boat on a lake. The scattering intensity of the wake and the frequency sequence at different times were studied [14]. The Dalian Institute of Measurement and Control Technology completed the sea test in 2006. The acoustic characteristics, width, depth, and section shape of the ship's wake were analyzed in a preliminarily study [15].

In summary, in China, the study of wakes started relatively late, and most of the research was conducted via simulation and laboratory research. No detailed sea test and analysis of the characteristics of ship acoustic wakes have been conducted.

Bubble dynamics is one of the most effective means of studying bubble wakes. Thus, in this study, starting from bubble dynamics, we investigated the motion of bubbles in the sea water under good hydrology and deduced the volume scattering intensity of the wake of the target with changes in frequency. Then, using high-performance test equipment, we conducted several sea tests on the target wake of a surface ship at typical frequencies, extracted the clear and stable acoustic characteristics of the acoustic wake, and subsequently developed a statistical model of target wake characteristics for target guidance and recognition of acoustic wake targets.

2. Acoustic Scattering Modeling of Bubble Wakes

According to the second law of thermodynamics, when a bubble is forced to vibrate, part of the sound energy is used to counteract the work done owing to the friction force of the bubble's vibration, which is released in the form of heat. This phenomenon leads to changes in the bubble's boundary conditions. The existence of bubbles will affect the nature of the medium of sound propagation and significantly affect the propagation speed of the sound wave [16]. Moreover, the sound velocity will also have a small imaginary part due to the absorption and scattering of sound waves, which will cause the exponential decay of sound intensity with propagation distance. Based on the variation in sound velocity, the ability of wakes to reflect incident sound wave is studied.

2.1. Acoustic Scattering Equation for a Group of Bubbles. When the sound wave is incident on the wake region, sound scattering is generated in the bubble, and mutual scattering between bubbles will also exist. The internal acoustic emission in the wake is represented by the scattering of the incident acoustic wave by the bubbles and by one or more scattering incidents from other bubbles. The sound waves are very weak after several successive scatterings; hence scattering between two or more bubbles can be neglected.

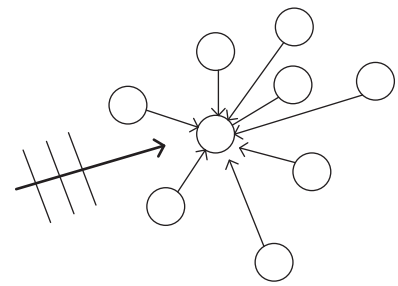

Figure 1: Scattering of bubbles.

As shown in Figure 1, for N bubbles, considering only primary scattering, the bubbles receive acoustic waves scattered from incident sound waves and other bubbles.

By Newton's laws of motion, the sound pressure equations [17] from the actual bubble are obtained. The equation of motion of the nth bubble is obtained as

$$m_n\ddot{v}_n + b_n\dot{v}_n + \kappa_n v_n = -P_n e^{i(wt+\phi_n)} - \sum_{j\neq n}^{N} \frac{\rho e^{-ikr_{jn}}}{4\pi r_{jn}}\ddot{v}_j \quad (1)$$

The equations of motion for all bubbles are expressed as

$$\begin{aligned} m_1\ddot{v}_1 + b_1\dot{v}_1 + \kappa_1 v_1 &= -P_1 e^{i(wt+\phi_1)} - \sum_{j\neq 1}^{N} \frac{\rho e^{-ikr_{j1}}}{4\pi r_{j1}}\ddot{v}_j \\ &\vdots \\ m_n\ddot{v}_n + b_n\dot{v}_n + \kappa_n v_n &= -P_n e^{i(wt+\phi_n)} - \sum_{j\neq n}^{N} \frac{\rho e^{-ikr_{jn}}}{4\pi r_{jn}}\ddot{v}_j \\ &\vdots \\ m_N\ddot{v}_N + b_N\dot{v}_N + \kappa_N v_N &= -P_N e^{i(wt+\phi_N)} \\ &\quad - \sum_{j=1}^{N-1} \frac{\rho e^{-ikr_{jN}}}{4\pi r_{jN}}\ddot{v}_j \end{aligned} \quad (2)$$

Among them, m is the mass of liquid, b is the damping coefficient, k is the stiffness coefficient of bubbles, ρ is the density of water, p is the amplitude of incident wave, and v is the difference of differential volume (the difference between instantaneous volume and equilibrium volume of bubbles).

2.2. Equivalent Sound Velocity of a Group of Bubbles. As $v_n = \overline{v}_n e^{iwt}$ [17], w is incident wave angular frequency; applying (2), the following forms can be obtained: MV=P.

Among them,

$$\begin{aligned} \mathrm{V} &= \{\overline{u}_1, \ldots, \overline{u}_n, \ldots, \overline{u}_N\}, \\ \mathrm{P} &= \{-p_1, \ldots, -p_n, \ldots - p_N\} \\ &= \left\{-p_1 e^{i\phi_1}, \ldots, -p_n e^{i\phi n}, \ldots - p_N e^{i\phi N}\right\} \end{aligned} \quad (3)$$

M is the N × N matrix:

$$M_{nn} = \kappa_n - \omega^2 m_n + i\omega b_n;$$
$$M_{nj} = \frac{w^2 \rho e^{-ikr_{jn}}}{4\pi r_{jn}} \quad (n \neq j). \tag{4}$$

It can be deduced from the equations that $M = M^T$, and the feature vector $\{u_n\}$, $\{\lambda_n\}$ is the characteristic value corresponding to the $\{u_n\}$,

$$Mu_n = \lambda_n u_n \tag{5}$$

V is represented as u_n V $= \sum_{n=1}^{N} c_n u_n$

Because u_1 represents the first scattering of bubbles, the effect is much greater than that of successive scatterings. This is reflected in the scattering equation; that is, when $n > 1$, we obtain $|c_1| \gg |c_n|$, c is the velocity of sound in water, and MV=P. Therefore,

$$\mathrm{MV} = \sum_{n=1}^{N} c_n M u_n = \sum_{n=1}^{N} c_n \lambda_n u_n = \mathrm{P} \tag{6}$$

For $n > 1$, $|c_1| \gg |c_n|$, only the first item is available: $c_1 = {u_1}^T p/\lambda_1$.

Suppose U is a symmetric matrix, then $UU^T = I$, $u_1^T u_1 \neq 0$, and therefore,

$$\langle v \rangle \approx \langle c_1 u_1 \rangle = \left\langle \frac{u_1^T p u_1}{\lambda_1} \right\rangle \tag{7}$$

It is assumed that the N bubbles are symmetrically distributed, i.e., the action angles between each pair of bubbles are the same; therefore,

$$u_1^T = \frac{1}{\sqrt{N}\,[111\ldots1\ldots1]\,u_n} \tag{8}$$

From (5), $\lambda_1 = u_1^T M u_1$

$$\lambda_1 = \left(\kappa_n - w^2 m_n + i\omega b_n\right) - w^2 \rho f \int_0^\infty r e^{-ikr} dr \tag{9}$$

Applied to (7), we find $\langle v_n \rangle = -F_n(1/N)\sum_n p_n/(1 - F_n w^2 \rho f_n \int_0^\infty r e^{-ikr} dr)$

$$F_n = \left(\kappa_n - \omega^2 m_n + i\omega b_n\right)^{-1} \tag{10}$$

f_n is the number of bubbles with a radius of a_n per unit volume.

Therefore

$$\frac{1}{c_m^2} = \frac{1}{c^2} + \frac{\sum_n \rho f_n F_n}{1 - \sum_n F_n w^2 \rho f_n \int_0^\infty r e^{-ikr} dr} \tag{11}$$

2.3. Scattering Strength of Real Bubbles. We assume that sound waves are coming from an infinite distance to the bubble layer, as shown in Figure 2.

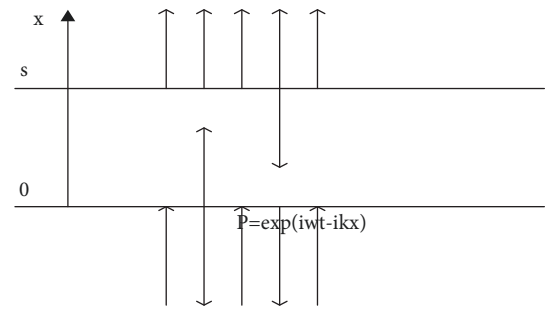

Figure 2: Sound propagation in layered media.

In x<0, there are incident waves and reflected waves, the amplitude of an incident wave is 1, and the amplitude of a reflected wave is A_-. The wave equation is [18]

$$P_-^0 - P_{-\infty} = \exp(iwt - ikx) + A_- \exp(iwt + ikx) \tag{12}$$

Only the transmission wave exists to the right x>s of the bubble layer, the amplitude of the transmitted wave is A_+, and the wave equation is

$$P_+^0 - P_\infty = A_+ \exp(iwt - ikx) \tag{13}$$

At $0 \leq x \leq s$, the wave equation in the bubble layer is denoted by

$$P - P_\infty = B_- \exp\left(iwt + ik_m x\right) + B_+ \exp\left(iwt - ik_m x\right) \tag{14}$$

where k_m is the equivalent wave number in the bubble layer, B_- is the incident wave in the bubble layer, and B_+ is the reflected wave in the bubble layer.

The phase velocity field in different layers can be expressed as

$$u = \frac{1}{iw\rho}\frac{\partial P}{\partial x} = \mp\frac{k}{w}\frac{P - P_\infty}{P} \tag{15}$$

Applying boundary conditions at x=0, we get

$$1 + A_- = B_- + B_+ \tag{16}$$

$$\frac{(1 - A_-)}{c\rho} = \frac{(B_- + B_+)}{c_m \rho} \tag{17}$$

Assuming that the bubble layer is very thick and that the sound wave cannot pass through the bubble layer, then

$$A_+ = B_- = 0 \tag{18}$$

By applying boundary condition equations (16), (17), and (18), we get

$$A_- = \frac{(c_m - c)}{(c_m + c)} \tag{19}$$

Therefore, the reflection coefficient of the bubble layer, R, is

$$R = \left|A_-\right|^2 \tag{20}$$

From the above statements, the scattering of group bubbles at a water depth of 2 m is calculated. When the volume

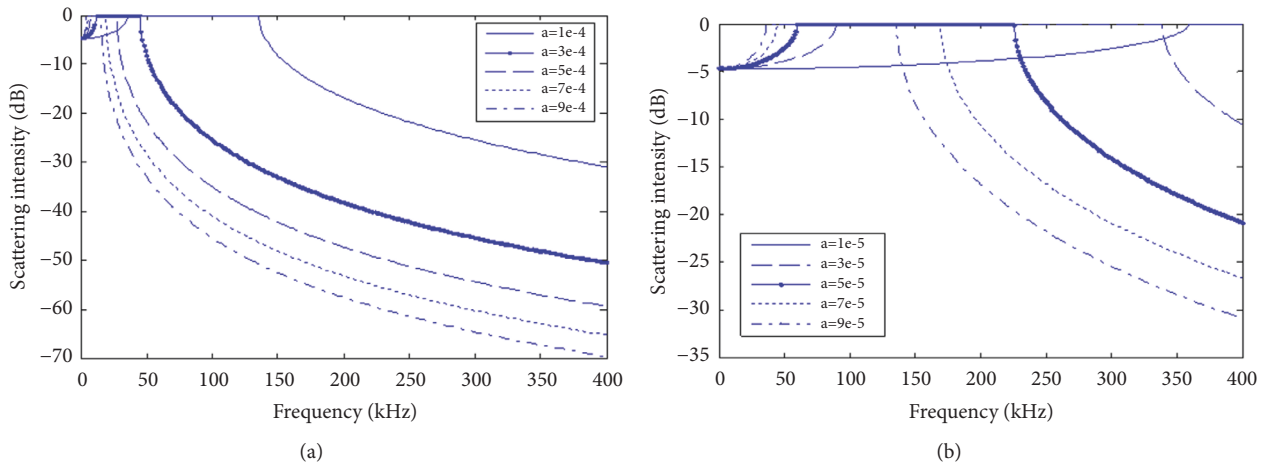

Figure 3: Scattering intensity of bubbles with different radii.

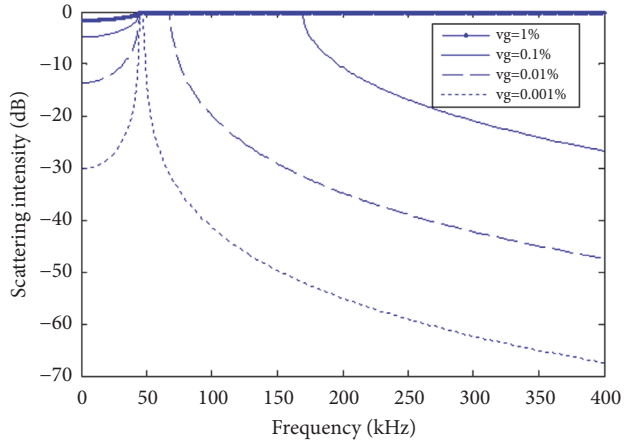

Figure 4: Relation between scattering intensity and volume fraction.

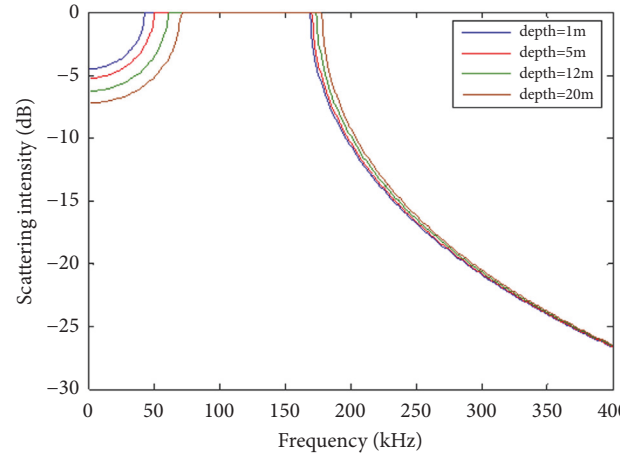

Figure 5: Relation between scattering intensity and depth.

fraction is 0.1%, the scattering intensities of the bubble groups of each radius are as shown in Figure 3. The results show that the scattering intensity of the bubble is related to the radius of the bubble, and the scattering intensity is larger near the resonance frequency. Parameter a is the radius of the bubble, the transverse axis is the incident frequency, and the longitudinal axis is the scattering intensity.

The bubble radius has an influence on the resonance frequency, and the scattering intensity varies with frequency. In the same volume fraction, the bubble radius is different, and the corresponding frequency response is also different. The most fundamental factor is the resonance frequency, and the scattering intensity is large near the resonance frequency.

At the same time, the volume fraction of air influences the scattering intensity. The larger the volume fraction, the greater the scattering intensity. Taking the bubble radius of 80 μm as an example, the depth scattering intensity of 2 m with volume fractions of 1%, 0.1%, 0.01%, and 0.001% is shown in Figure 4. The volume fraction is VG, the transverse axis is incident frequency, and the longitudinal axis is scattering intensity. At the same frequency, the greater the volume fraction, the greater the scattering intensity.

The volume scattering strength of group bubbles with a bubble radius of 80 μm and a volume fraction of 0.1% at depths of 1 m, 5 m, 12 m, and 20 m is shown in Figure 5. The transverse axis is incident frequency, and the longitudinal axis is scattering intensity shown for different color-coded depths. It can be observed that when incident frequency is less than the resonant frequency, there is a good relationship with the depth of the bubble scattering intensity group, and with increasing depth, the scattering intensity decreases. When the incident frequency is greater than the resonant frequency, the scattering intensity has a weak relationship with depth.

2.4. Volume Scattering Strength of Wakes. The number, density, and distribution of bubbles in the wake of a ship are related to the geometric characteristics of the wakes, as well as the buoyancy, velocity and the dissolution of the bubbles. As the bubbles from the hull and propeller leave the ship, large bubbles will break or float soon afterwards. The minuscule

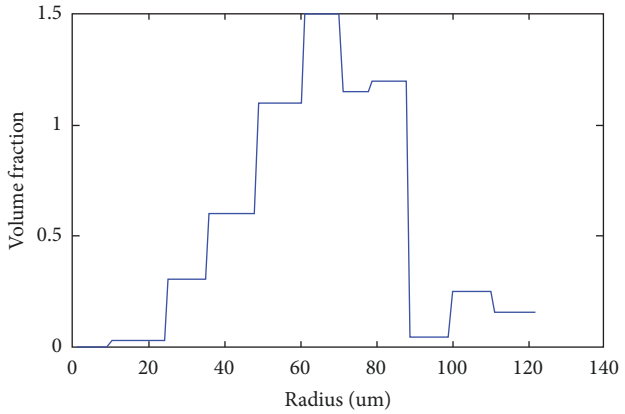

Figure 6: Bubble distribution in wake.

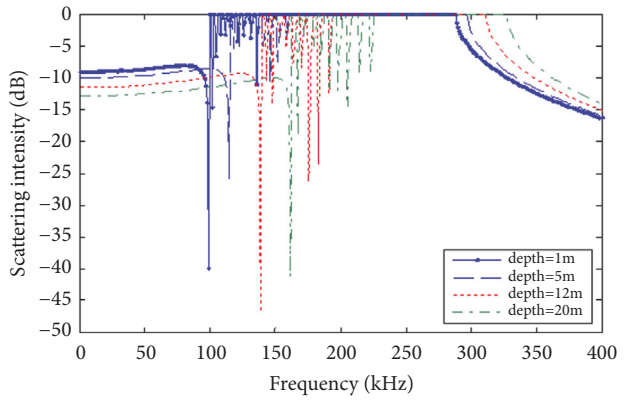

Figure 7: Volume scattering strength of wakes.

bubbles will disappear because of dissolution. Only 10 – 300μm bubbles are left in the wake. There are many methods [19] for studying bubble distribution, but the distribution of bubbles in wakes is a military secret. The scattering intensity of the wake, as shown in Figure 7, can be calculated by using the bubble distribution rule shown in Figure 6 [20].

From the calculation results, the scattering intensity of the wake is related to the emission frequency, which is due to the resonant frequency effect of the bubble. When the incident frequency is less than the resonance frequency of most of the bubble, the volume scattering intensity decreases with the increase in depth. However, when the incident frequency is greater than the resonant frequency of most of the bubble, the scattering intensity increases with the increase in depth.

2.5. Comparison of Theoretical Modeling Results with Actual Data Analysis Results. In 2013, the frequency characteristics of the wake scattering of a landing craft in the Dalian black mouth wharf bay were tested. Figure 8 shows the results of the measurement of the volume scattering intensity of the multifrequency single beam sonar simultaneous base test. The speed is 7 kn.

The test results show that the volume scattering intensity of the ship wake is related to frequency, depth, and air content, and is consistent with the theoretical trend. The measured

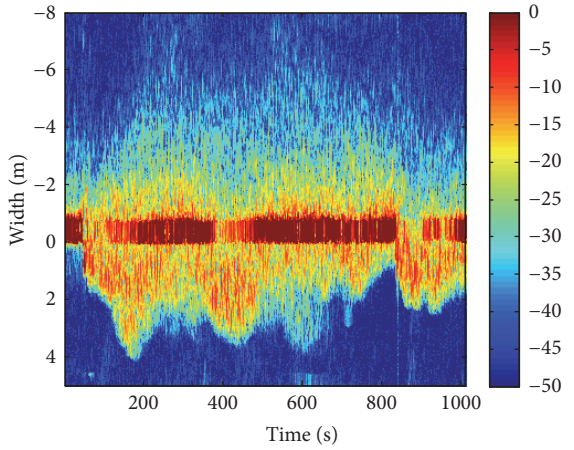

Figure 8: Volume scattering strength of the wake.

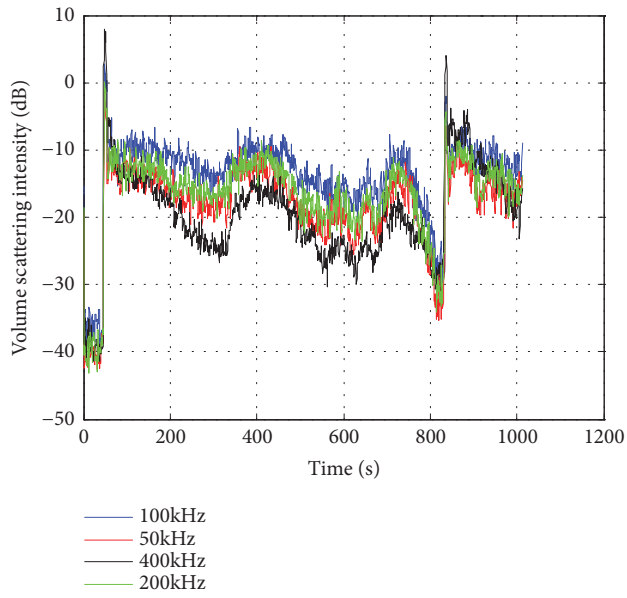

Figure 9: Volume scattering strength of wake volume at 1 m.

volume scattering intensity is about 10 dB smaller than the theoretical prediction. From Figure 9, we observe that there are obvious multiple reflections between wake bubbles. While simulation modeling ignores mutual scattering two times and above between bubbles, this may be the main reason for the strength deviation of the measured volume scattering intensity. At the same time, because the actual bubble scattering is more complex, there are many influencing factors. There is a large deviation between the scattering intensity near the resonance frequency and the actual wake, and the resonance response under the actual condition is restricted by many factors, such as acoustic absorption.

3. Experimental Details and Results

Based on the experimental study of theoretical calculation and terminal verification, the test equipment is placed under

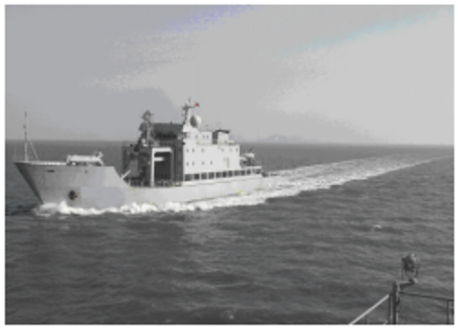

Figure 10: Target ship.

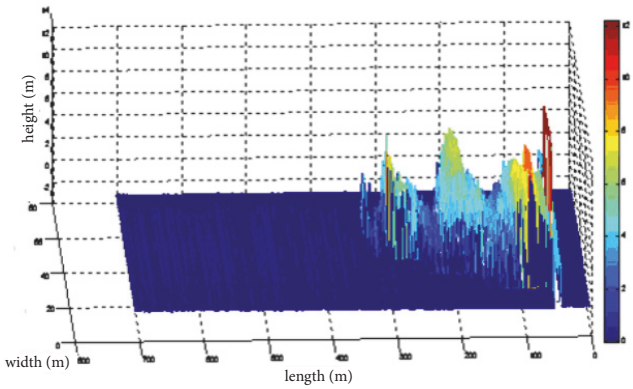

Figure 11: 3D process chart of target ship.

the wake of the ship. We used the dual frequency multibeam sonar to carry out a multivoyage test, and tried to obtain the characteristics of a specific state by multiple measurements. The characteristics of 100 kHz wake and the stable statistical model under this condition were obtained.

3.1. Test Survey. In 2013, the discharge characteristics of 2200T civil ship's wake acoustic scattering were tested in the sea near the Three Islands in Dalian. The sea state was 2–3 levels during the test. Figure 10 shows the target ship. Figure 11 shows a three-dimensional flow chart of the wake of the target ship. The Z-axis is the depth of the bubble wake and 0 m is the water surface.

3.2. Feature Extraction and Statistical Model

3.2.1. Parameter 1: Maximum Volume Scattering Intensity, S. The volume scattering intensity of the wake is generally less than -10 dB, and it decreases with time. As the speed increases, the scattering intensity increases. The noise interference of the propeller, the bottom, and the wake of the ship can be observed in Figures 12(a) and 12(b). The wake bubbles created right after the propeller started had large size and high density, so the scattering intensity is very strong. Because of propeller and hull vortex and the floating of large bubbles, the wake flow rapidly rises to the surface of the sea. With the rupture of large bubbles and the mixing of the sea water beyond the hull, the broken bubbles gradually spread to the four sides. Therefore, the wake depth tends to increase, and the intensity gradually decreases. From Figures 12(c) and 12(d), it can be observed that, at high speed, the volume scattering strength of the underwater of 1 m is clearly reduced at the initial stage of the wake. It is possible that the strong wake generated by the propeller blocks the sound energy, and or that the hole area produced by the liquid gasification near the propeller. This issue needs further study.

3.2.2. Parameter 2: Intensity Ratio to the Sea Surface Signal, T. According to the characteristics of the sound reflection of the longitudinal section of the bottom of the ship, Q1 is the signal intensity before the sound wave reaches the sea surface, Q2 is the signal intensity after the sound wave reaches the sea surface, and $T = 20\times\log_{10}(Q_1/Q_2)$ is the curve of the intensity ratio between the ship bottom wake and the sea surface.

As can be seen in Figure 13, the T >12 dB is the bottom of the ship, the -30 dB< T <12 dB is the wake, and the T< -30 dB is the sea surface. Whether the target ship is at high speed or low speed, the bottom of the ship is T>12 dB, and the sea surface has T<-30 dB, which has strong consistency. When the speed is 13 kn, the T value is larger, which may be related to the weaker acoustic signal reaching the sea surface. However, the difference between the T value of the wake and the bottom is still greater than 10 dB.

3.2.3. Parameter 3: Steepness of the Echo Signal, G. The "steepness" of the echo signal is defined as the ratio of the amplitude to the time between the starting point of the wake signal and the peak value of the signal. For the high frequency incident signal, the bottom of the ship can be regarded as an "absolutely hard" medium. The reflected signal is usually the same as the frequency of the incident signal, the signal intensity is large, the peak fluctuation of the signal is small, and the signal envelope is similar to the incident signal. The ship's wake contains a large number of bubbles of different sizes. The scattering signal is the superposition of the effects of each bubble, the peak fluctuation of the signal is very large, and the frequency fluctuation of the signal is relatively large. Therefore, the bottom signal and the wake signal steepness have obvious differences, as shown in Figure 14.

3.2.4. Parameter 4: Mean Square Deviation Corresponding to the Maximum Value of the Signal, σ. In Figure 15, it can be seen that the echo depth of the bottom part, the sea surface, and the wake have different regularities. The largest fluctuation of the signal maximum value of the flat part of the ship's bottom is smallest, the sea level is second largest, and the wake fluctuation is the largest. At low- and high-speed voyages, the mean square deviation of ship bottom flatness, sea surface, and wake signals are 0.09 m, 0.1 m, and 1.4 m (low speeds) and 0.07 m, 0.09 m, and 1.6 m (high speeds), respectively.

3.2.5. Parameter 5: Correlation Coefficient Intensity ρ. At the beginning of the wake, the copy characteristics are relatively strong, and this is not related to the ship type. However, the internal heterogeneity of the wake causes the fluctuation

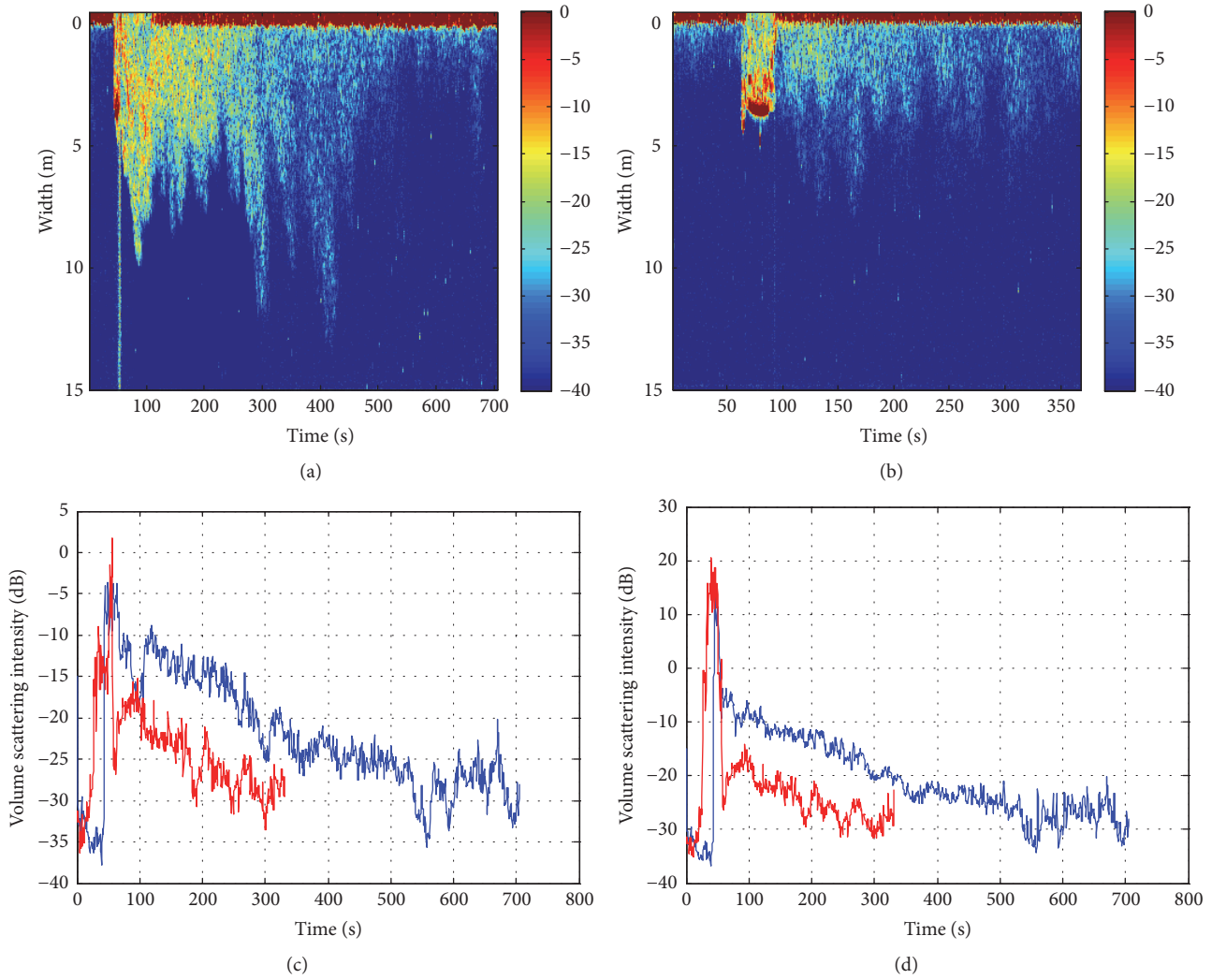

Figure 12: Volume scattering strength (a) 13 kn; (b) 5 kn; (c) 1 m; (d) maximum.

of the copy correlation coefficient, and there is no obvious relationship with the depth. When the wake is formed for a period of time, the copy correlation characteristics rapidly decrease, which is caused by the rapid diffusion of bubbles and the separation of bubble masses. As shown in Figure 16, the copy correlation of the wake is gradually reduced. Although the wake echo is the common effect of the scattering of a large number of bubbles, the phase change of the echo is not very strong and is irregular at the beginning of the wake. The irregular scattering of the bubbles inside the wake does not exert a great influence on the wake echo.

3.2.6. Parameter 6: Mutation Times N. Wavelet transform can detect the edge hopping of the signal. Because of the fluctuation of bubbles in the wake and the scattering and absorption of bubbles, a large number of wavelets will be generated by the reflection sound wave, and there will also be many fluctuation jitters of each subwave. Consequently, the frequency of mutation and fluctuation of the received signal will also be high. The echo of the ship bottom and the sea surface is basically caused by the mirror reflection. The bottom of the ship is stronger than the sea surface, and the sea surface has some irregularity, so there is little difference between the echo envelope and the fluctuation frequency of the ship bottom and the sea surface. The db1 wavelet decomposition is used to process the three levels of detail information, and the number of the first extreme points of the first derivative is counted, which is the number of echo signal mutation times, in order to distinguish between the wake, the sea surface, and the bottom signal.

The number of mutations obtained using wavelet transform to detect the signal is shown in Figure 17. The statistical results can be seen in the figure: the wake echo signal has the most mutations, and the number of sea surface and bottom echo signal mutations do not differ significantly, which is consistent with the results of our theoretical analysis.

Based on the statistical analysis of the test data, the following statistical models (Table 1) were obtained.

3.3. Wake Hole. A clear hole phenomenon was found in the vertical image of the wake echo, as seen in Figure 18. The

Table 1: Target feature statistics table.

	bottom	wake	Sea surface
Maximum unit volume scattering intensity S (dB)	S > -5	-40 < S <-5	S < -40
Intensity ratio to the sea surface signal T (dB)	T >12	-30 <T<12	T< -30
Steepness of the echo signal G (V/s)	G>2000	G<500	2000>G>500
Mean square deviation corresponding to the maximum value of the signal σ (m)	$\sigma < 0.2$	$\sigma > 1.0$	$\sigma < 0.2$
Correlation coefficient intensity ρ	$\rho > -20$	$-65 < \rho < -20$	$\rho < -70$
Number of mutations in the signal envelope N (Times)	N<200	N>300	N<200

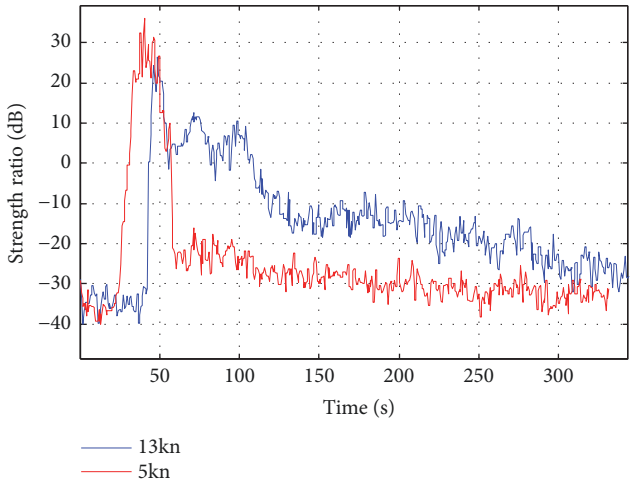

Figure 13: Ratio of ship bottom flow to sea surface signal intensity.

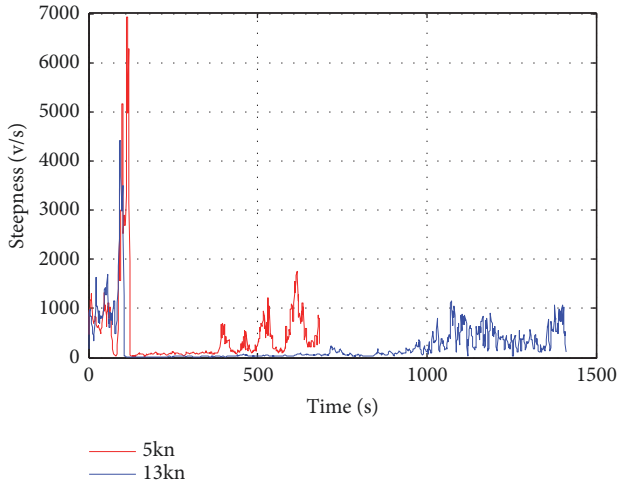

Figure 14: Ship bottom, wake, and sea surface signal steepness.

gap in the image may be holes, or it may be a diffusion separation of the wake. Further studies are needed to explain such cavities.

4. Conclusions

Considering the results presented in the previous section, the following conclusions can be drawn:

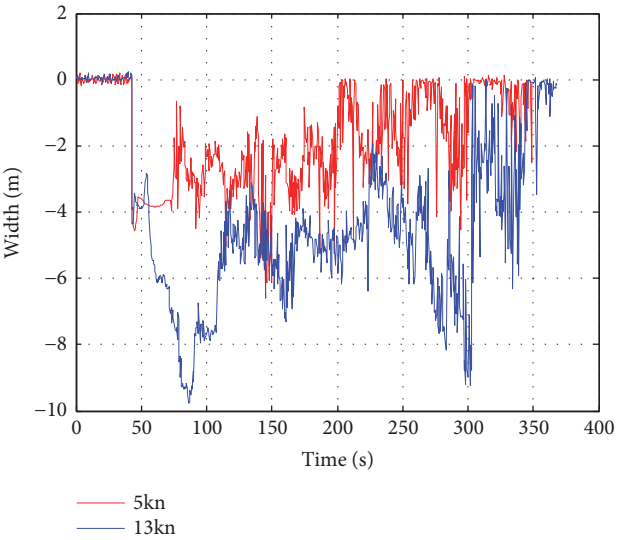

Figure 15: Ship bottom, wake, and sea surface depth change.

(1) The relationship between the wake volume scattering intensity and the frequency is consistent with the theoretical trend. Nevertheless, the measured volume scattering intensity is about 10 dB smaller than the theoretical prediction. The experimental study shows that there are obvious multiple reflections among the wake bubbles, while in the simulation modeling the mutual scattering of bubbles between two and above is neglected. This may be the main reason for the strength deviation of the measured volume scattering intensity. At the same time, due to the fact that the actual bubble scattering is more complex and the influence factors are more than accounted for, the scattering intensity near the resonance frequency is larger than the actual wake. This is due to the fact that there are many factors in the wake scattering, and the resonance response under the actual condition is restricted by many factors, such as sound absorption.

(2) On the basis of statistical analysis of the data, a six-parameter statistical model of ship wake characteristics is established for a specific ship type, in which the maximum unit volume scattering intensity, intensity ratio to the sea surface signal, steepness of the echo signal, mean square deviation corresponding to the maximum value of the signal, correlation coefficient intensity, and the number of mutations in the signal envelope are used as inputs. It can be used as a recognition criterion for ship wake. However, due to the

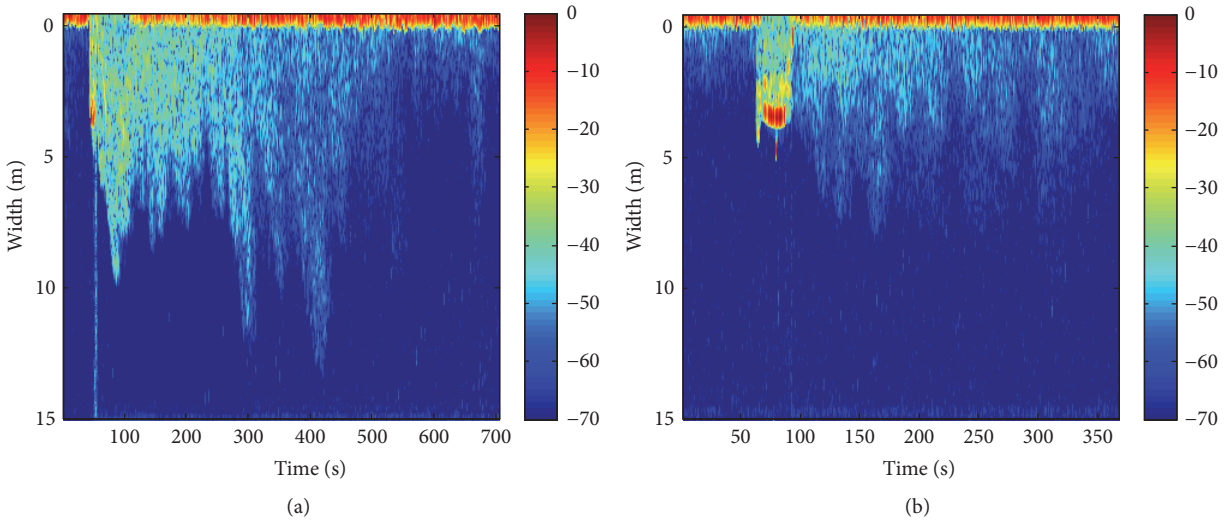

Figure 16: Copy correlation characteristics: (a) 13 kn; (b) 5 kn.

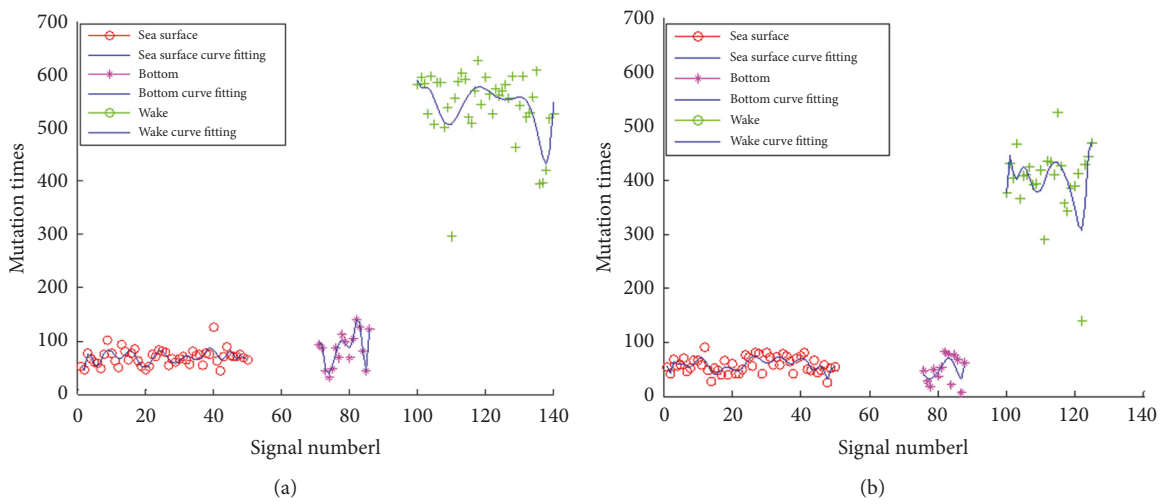

Figure 17: Frequency of signal mutation: (a) 13 kn; (b) 5 kn.

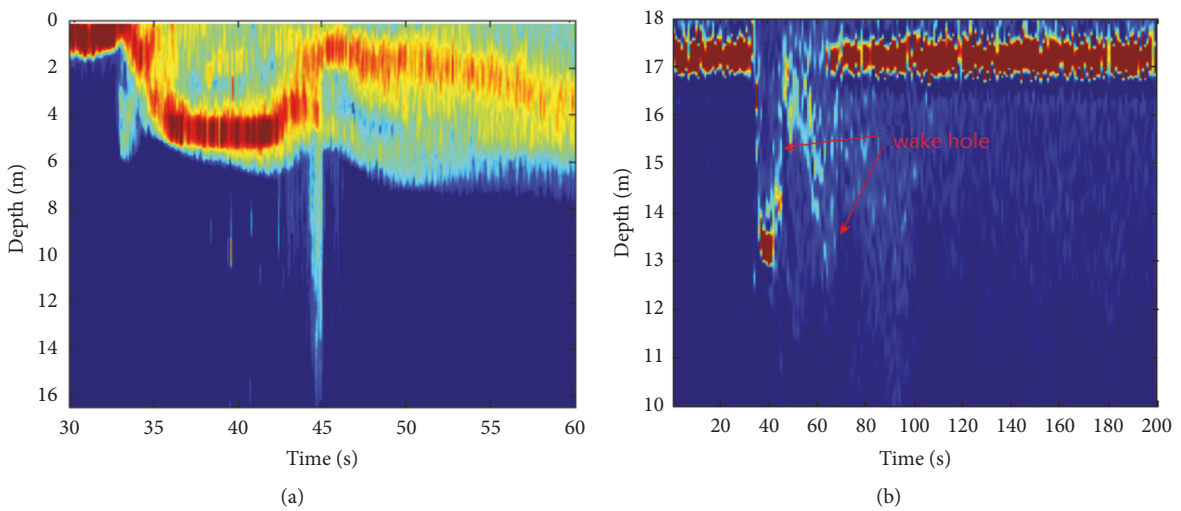

Figure 18: Wake acoustic scattering image: (a) local; (b) the whole.

fact that the actual bubble scattering is more complex and the influence factors are more than accounted for, it still needs further study to establish a general statistical model suitable for a variety of ship types.

(3) In the sea test, the longest duration of the wake of the multibeam sonar is more than 30 minutes, which is the longest duration of the ship sound wake in China. The duration of the wake is related to the ship type, velocity, the direction of the ocean current, and the testing capacity of the test equipment. However, in the sea trial, the direction of ocean current and the testing ability of the test equipment are more influential.

(4) The blankness in the wake may be a wake hole or the diffusion separation of the wake. These experiments provide directions for further understanding of wake and further research on the characteristics of wake.

Data Availability

All data used to support the findings of this study were supplied by Dalian Scientific Test and Control Technology Institute, Dalian 116013, China, under license and so cannot be made freely available. Requests for access to these data should be made to first author and correspondence author.

Conflicts of Interest

The authors declare that there are no conflicts of interest regarding the publication of this paper.

Acknowledgments

This research project is supported by the National Key Basic Research Development Program, Science and Technology on Underwater Test and Control Laboratory, "13th Five-Year" Field Fund [Grant no. 61404160301], and the National Natural Science Foundation of China [Grants nos. 61371171 and 61501061].

References

[1] J. Xingzhoui, "Analysis of operational effectiveness of Jiang Xingzhou 53-65 K wake guided torpedo," *Torpedo Technology*, vol. 8, no. 1, pp. 37–41, 2000.

[2] G. A. Garrettson, "Bubble transport theory with application to the upper ocean," *Journal of Fluid Mechanics*, vol. 59, no. 1, pp. 5–1973, 1973.

[3] M. B. Stewart and E. W. Miner, *Bubble dynamics in a turbulent ship wake*, US:NUL-MR-6055, 1987.

[4] E. W. Miner and S. E. Ramberg, *Method for approximating the initial data plane for surface wake simulation*, US:NRL-MR-6376, 1988.

[5] P. M. Carrica, D. Drew, F. Bonetto, and R. T. Lahey Jr., "A polydisperse model for bubbly two-phase flow around a surface ship," *International Journal of Multiphase Flow*, vol. 25, no. 2, pp. 257–305, 1998.

[6] E. L. Carstensen and L. L. Foldy, "Propagation of Sound Through a Liquid Containing Bubbles," *The Journal of the Acoustical Society of America*, vol. 19, no. 3, pp. 481–501, 1947.

[7] E. Silberman, "Sound Velocity and Attenuation in Bubbly Mixtures Measured in Standing Wave Tubes," *The Journal of the Acoustical Society of America*, vol. 29, no. 8, pp. 925–933, 1957.

[8] M. Zhongcheng, "Study on sound characteristic measurement system and the ship testing of ships wake," *Underwater Target Feature, Dalian*, pp. 37–39, 2002.

[9] Z. Shihong, W. Zhicheng, and W. Rongqing, "Foreign underwater military target characteristic research dynamic level and equipment demand analysis," *China national science and technology report*, pp. 120–125, 2002.

[10] S. Shengwei and J. Xingzhou, "Study on the motion characteristics of ship wake bubbles," *Journal of Wuhan University of Technology*, vol. 31, no. 5, pp. 219–221, 2007.

[11] D. Nie, J. Lin, L. Qiu, and X. Zhang, "Lattice Boltzmann Simulation of Multiple Bubbles Motion under Gravity," *Abstract and Applied Analysis*, vol. 2015, Article ID 706034, 12 pages, 2015.

[12] Z. Donghua and Z. Xiaohui, "Numerical calculation of ship wake and its bubble number density distribution," *Journal of Ordnance Industry*, vol. 32, no. 3, pp. 315–317, 2011.

[13] Z. Qun and W. Yingmin, "Structural static analysis of bubbles in ship wake," *Computer Simulation*, vol. 31, no. 9, 2014.

[14] C. Ping and Z. Daizhu, "Experimental study on acoustic scattering of surface ship wake," *Acta Acoustics Sinica*, vol. 1, pp. 1–6, 2000.

[15] D. Jinglin, M. Zhongcheng et al., "Experiments on acoustic scattering and geometric characteristics of ship wake," *Journal of HarbinEngineering University*, vol. 31, no. 7, 2010.

[16] P. M. Carrica, D. Drew, F. Bonetto, and R. T. Lahey Jr., "A polydisperse model for bubbly two-phase flow around a surface ship," *International Journal of Multiphase Flow*, vol. 25, no. 2, pp. 257–305, 1999.

[17] M. V. Hall, "A comprehensive model of wind-generated bubbles in the ocean and predictions of the effects on sound propagation at frequency up to 40 kHz," *The Journal of the Acoustical Society of America*, vol. 99, pp. 169–208, 1996.

[18] G. V. Norton and J. C. Novarini, "Enhancement of the total acoustic field due to the coupling effects from a rough sea surface and a bubble layer," *The Journal of the Acoustical Society of America*, vol. 103, no. 4, pp. 1836–1844, 1998.

[19] S. Hampton, *Acoustic Bubble Density Measurement Technique for Surface Ship Waters*, A Thesis, Naval Postgraduate School, AD-A187 967/5/HDM, 1987.

[20] R. Duraiswami, S. Prabhukumar, and G. L. Chahine, "Bubble counting using an inverse acoustic scattering method," *The Journal of the Acoustical Society of America*, vol. 104, no. 5, pp. 2699–2717, 1998.